

PAPER • OPEN ACCESS

Numerical analysis of the hydraulic force of a pump turbine under partial load conditions in turbine mode

To cite this article: L K Wang *et al* 2019 *IOP Conf. Ser.: Earth Environ. Sci.* **240** 072041

View the [article online](#) for updates and enhancements.

You may also like

- [Evolution and influence of high-head pump-turbine cavitation during runaway transients](#)

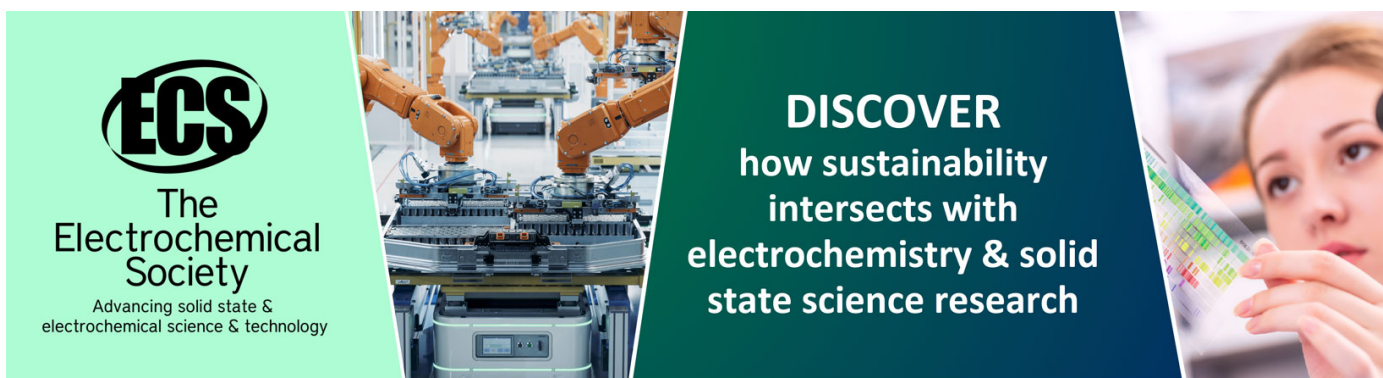
W D Wu, K Liu, L Li *et al.*

- [The Greenland Norse and the little ice age: Large scale climate changes to a small scale society](#)

Niels Lynnerup, J Arneborg, J Heinemeier *et al.*

- [Dynamic Radial Forces and Pressure Fluctuations Measurement at Off-Design Conditions on a Model Scale Pump-Turbine](#)

V Novotný, V Habán, A Skoták *et al.*



ECS
The
Electrochemical
Society
Advancing solid state &
electrochemical science & technology

DISCOVER
how sustainability
intersects with
electrochemistry & solid
state science research

Numerical analysis of the hydraulic force of a pump turbine under partial load conditions in turbine mode

L K Wang¹, J L Lu¹, W L Liao¹, Y P Zhao¹, Q F Ji¹

¹Institute of water Resource and hydro-electric Engineering, Xi'an University of Technology, Xi'an, China

E-mail: jinling_lu@163.com

Abstract. The power grid demand keeps changing at any time, so the pump turbine often operates in partial load condition. The noise and vibration of the unit caused by hydraulic force have an adverse effect on the safe and stable operation of the power plant. In order to study the mechanism of hydraulic force, a model pump turbine of a pumped-storage power station was set as the research object in this paper, both the steady and unsteady numerical simulation were carried out to simulate the flow field and hydraulic force of pump turbine. Axial force will increase significantly when the unit overloaded, but it has almost no change at partial load conditions. And the axial force on the runner is mainly produced by the hub and shroud, while it can be ignored on the blade. The radial force increases sharply when the condition deviates from the rated operating point. The frequency of pressure fluctuation is $20f_n$ which is caused by rotor stator. There is more low frequency pressure fluctuation at small discharge condition because of the flow separation. The amplitude and deviation coefficient increased. The heterogeneity of pressure pulsation leads to the increase of radial force at partial load condition.

1. Introduction

With the fast development of new energy such as solar power and wind power, the proportion of new energy in the power grid is increasing. It will adversely affect the safety and stability of the power grid, because of the obvious instability and intermittent which influenced by the environment ^[1]. The pumped storage power plant has flexible operation ability, fast starting, real-time tracking of load change, so it is an indispensable tool to respond rapid changes and to realize optimal dispatching of power grid ^[2]. The pump turbine often operates in partial load condition. And the hydraulic force will significantly increased compared to the optimal condition. It will cause the unit severe vibration and affect the stable operation of the unit.

Among the forces on the reversible pump turbine, there are three kinds of excitation forces according to their origins: the hydraulic forces, the mechanical forces and electromagnetic forces ^[3]. What the present paper focuses on is hydraulic force. J W Li ^[4] found that the axial force is prominent in the turbine mode while the radial force is the dominant near the runaway and turbine break modes. The component perpendicular to the shaft caused by the asymmetric flow inside runner is the dominant one in runaway and turbine break regions. The runner is subjected to an asymmetric radial force whose amplitude varies periodically, the number of cycles are equal to the number of blades, The double-rotation stall phenomenon appears in the runner, and the stalls can impact on blades intermittently, resulting in an additional alternating stress on the blades ^{[5][6]}. The abnormal hydraulic force affects the safe operations of the pumped storage power station seriously. Such as,



Tianhuangping pumped storage power station, the frequent lifts of the rotational components of the reversible pump turbines were observed during the load increment from 200 MW to 300 MW in the generating mode, leading to the abrasive damage of the machine and hence unplanned closing down of the machine [7]. The literature review shows that the hydraulic force of the pump turbine runner under partial load conditions in turbine mode remains an issue to be explored.

2. Mathematical Model

2.1. Turbulence model

In this paper, the SST turbulence model was used to close the Reynolds averaged Navier–Stokes (RANS) solver for the solution of the turbulence flows. The continuity equation and momentum equation are adopted in simulation.

Continuity equation

$$\frac{\partial(\rho u_i)}{\partial x_i} = 0 \quad (1)$$

Momentum equation

$$\rho \frac{Du_i}{Dt} = \rho F_i - \frac{\partial p}{\partial x_i} + \frac{\partial}{\partial x_j} \left[\mu \left(\frac{\partial u_i}{\partial x_j} + \frac{\partial u_j}{\partial x_i} \right) \right] + \frac{\partial}{\partial x_i} (\lambda \nabla \cdot \mathbf{v}) \quad (2)$$

2.2. Compressible model

In engineering application, given the constant temperature and the compressibility of water is always represented by the bulk modulus of elasticity. The water density is defined as:

$$K = dp / (d\rho / \rho) \quad (3)$$

$$K = (p - p_0) / ((\rho - \rho_0) / \rho) \quad (4)$$

$$\rho = \rho_0 / \left(1 - \frac{p - p_0}{K} \right) \quad (5)$$

Where p is the static pressure and ρ is the density of water and K is the modulus of elasticity.

Under the operating conditions for hydraulic machinery, the modulus of elasticity can be assumed to be constant. In the present study, $K=2 \times 10^9$ Pa, $p_0=101325$ Pa and $\rho_0=998$ kg/m³. By means of user defined function, the variable sound speed is linked to the flow solver CFX.

3. III. NUMERICAL MODEL AND COMPUTATIONAL METHODS

3.1. Pump Turbine Specification

As shown in Figure 1, the whole pump turbine configuration including spiral case, stay vane, guide vane, runner and draft tube is considered in the physical model. Specifications of the pump turbine are listed in Table.1.

Table 1. Main specifications of pump turbine

Parameters	value
Runner blade number ZB	9
Guide vane number ZG	20
Stay vane number ZS	20
Experimental rotational speed (rpm)	750
Runner diameter at inlet D1(mm)	468
Runner diameter at outlet D2(mm)	300
Experimental head H(m)	20
Specific speed(r/min)	189

3.2. Grid generation

Mesh generation is an important component of numerical discretization in flow governing equations, mesh quality has a crucial impact on calculation accuracy. Structured hexahedral grid was used in this study to discretize all components in the ANSYS ICEM software. Grid quality values in ANSYS ICEM usually range from 0 to 1, with a higher grid value representing higher grid quality. Grids of all components details are shown in Figure 2.

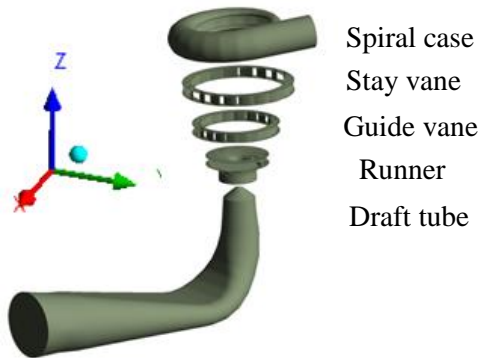


Figure 1. Three-dimensional model of the pump turbine

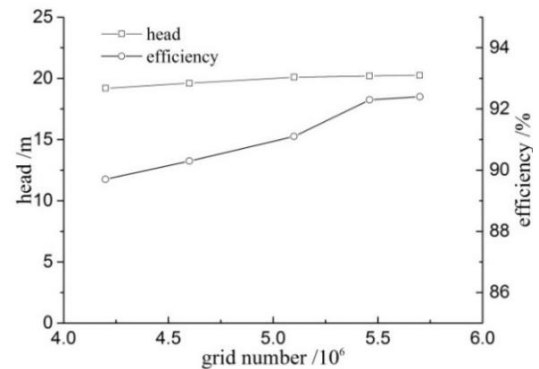


Figure 2. Mesh independence

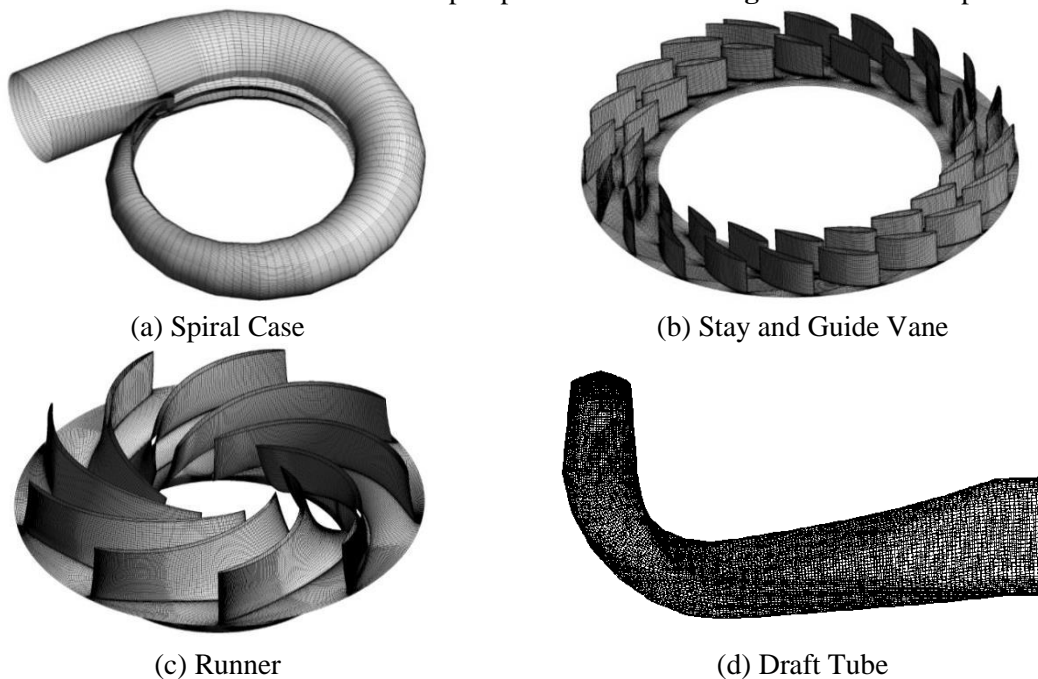


Figure 3. Grids of different components

Five mesh densities with increasing mesh size were used for the steady flow calculations under design condition to test for independence. Figure 3 shows the efficiency and head of the pump turbine from the simulations for the five different grid nodes. The total number of grid elements used was about 5.46 million, while the mesh for each component is shown in Table 2.

Table 2. The grid number of the computational domain

	Spiral case	Stay vane	Guide vane	Runner	Draft tube	total
Mesh number(*10 ⁶)	0.26	1.05	1.45	1.80	0.8	5.46

3.3. Boundary condition

- (1) **Inlet condition.** The mass flow inlet at the spiral case of pump turbine is used.

(2) **Outlet condition.** Pressure outlet is used at the draft tube of pump turbine, static pressure is specified for all cases.

(3) **Other boundary conditions.** No-slip condition has applied on the all solid walls, and standard wall function is used to calculate the turbulence kinetic energy and turbulence dissipation frequency near the wall.

(4) **Time step.** During the numerical simulations, the results of steady RANS simulations were used as the initial flow field for the transient simulations. Vlad Hasmatuchi^[8] compared unsteady numerical results of the three time steps that runner rotated 2, 1, 0.5 degree spent and argued that the time step which runner rotates 1 degree is reasonable in terms of computation time and accuracy. So the time that runner rotated 1 degree spent is adopted as the time step.

3.4. Calculation conditions

The numerical simulation of inflow pattern in pump turbine at different conditions was calculated in this paper is shown in Table.3. For convinence the operating conditions are plotted using unit parameters, which for hydro-turbines are defined as follows. The unit speed and unit flow rate is

$$n11 = nD / \sqrt{H} \quad (6)$$

$$Q11 = Q / D^2 \sqrt{H} \quad (7)$$

Where D is runner diameter at low pressure side, H is the net head across the pump turbine, n is the speed of runner in rpm and Q is the volume flow rate in m^3/s .

Table 3. Calculation condition points

Calculation points	Guide vane opening θ ($^\circ$)	$n11$ (rpm)	$Q11$ (l/s)	Loads (%)
OP1	16	63	480	55
OP2	18	63	570	70
OP3	20	63	635	80
OP4	22	63	700	90
OP5	24	63	755	100
OP6	28	63	850	110

4. Calculation results and Discussion

4.1. Hydraulic force

In order to analyse the radial force and axial force characteristic of pump turbine, a dimensionless parameter K is defined as follow^[9]:

$$K = \frac{100F}{0.5\rho u_1^2 \pi D_1 b_1} \quad (8)$$

where F is the radial force F_{xy} or axial force F_z , ρ is the density of water, u_1 , D_1 and b_1 are the circumferential velocity, diameter and width of runner inlet respectively.

The variation of axial force K_z and radial force K_{xy} under different working conditions from steady calculation results are as shown in Figure 4, It can be found that the axial force will increase significantly when overloaded, which is 6.7% higher than OP5. At the large flow condition, the differential pressure between the pressure and suction surface increases because of the rise of the blade load. This is the fundamental reason which leads to the increase of axial force. As the flow rate decrease, and the axial force almost has no change at partial load condition.

For the radial force, it is very small at the rated operating point and radial force coefficient K_{xy} is equal to 0.165. When the condition deviates from the rated operating point, K_{xy} increases sharply. The radial force coefficient K_{xy} is equal to 17.1 at OP1 and it is 103 times than rated operating point. At small flow condition, there is a positive angle of the runner inlet, which causes the flow separation on

the impeller pressure surface easily, and the smaller the flow rate is, the more serious the flow separation phenomenon is. At the same time, the inlet flow separation will affect the circumferential pressure distribution of the wheel inlet pressure, which makes the radial force increase sharply.

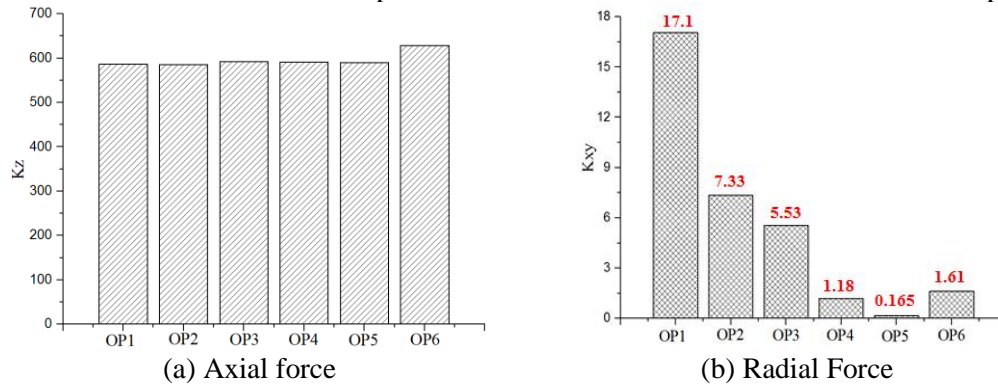


Figure 4. The variation of radial force K_{xy} and axial force K_z of the runner

As shown in Figure 5, it can be clearly seen that the distribution of pressure at OP5 is uniform. There are 9 peaks along the circumferential direction which is equal to blade number. The range of pressure fluctuation increased obviously when the working condition deviates from rated condition. For example at OP6, the maximum pressure is largest and the minimal pressure is smallest than other condition. Especially there is a low pressure area at OP1. In addition, the law of pressure distribution along the Span direction is also different. Those phenomena are the main reason that resulting in the increasing of radial force.

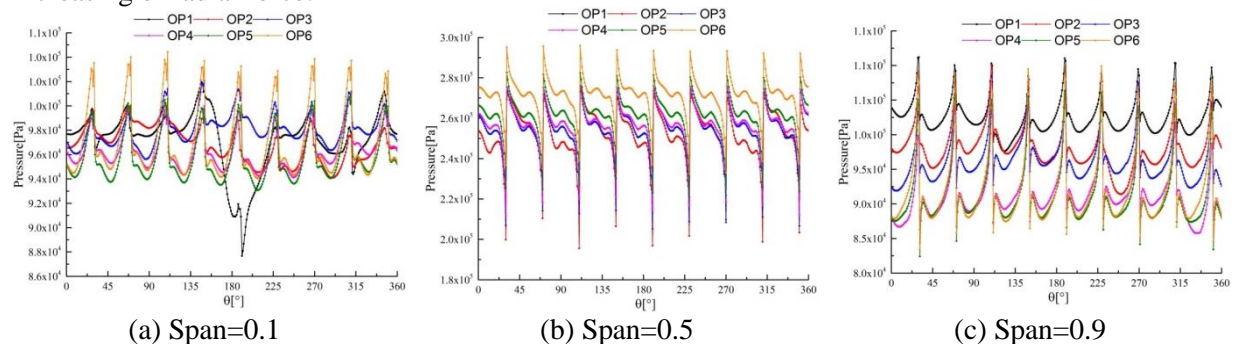


Figure 5. Circumferential pressure distribution of runner inlet

4.2. Hydraulic force pulsation characteristics

In order to ensure the accuracy of the calculation results, the data after 10 revolutions is analysed. The distribution of radial force with the rotation of the runner is shown in Figure 6. It can conclude that, the runner rotated almost four revolutions but one revolution of radial force at OP1, and the radial force shows the characteristics of high frequency fluctuation at OP4. Figure 7 shows the vector distribution of radial force. The coordinates of each point indicate the size and direction of the radial force. The radial force acting on the runner at different conditions is always changing and regularly distributed. The radial force is very small in the rated condition, but the value is not zero, which is deviated from the theoretical value. The flow inside the impeller is not completely symmetrical due to the asymmetry structure of the pump turbine. It will result in uneven distribution of velocity and pressure. The angle of runner inlet increases with the decrease of flow rate, and the radial force increases significantly.

4.3. Pressure fluctuation

The dimensionless number C_p (pressure fluctuation coefficient) is introduced in the treatment of pressure fluctuation data of various monitoring points, the definition of C_p as shown in equation (6), it

represents the percentage of pressure fluctuation in head size. And S is the dispersion coefficient and it represents the dispersion of pressure fluctuation amplitude.

$$C_p = \frac{\Delta P}{\rho g H} \times 100\% \tag{6}$$

$$S = \frac{|C_p - \bar{C}_p|}{\bar{C}_p} \tag{7}$$

Where $\Delta P = P - \bar{P}$ is the amplitude of pressure fluctuation, P is the pressure of numerical simulation, \bar{P} is the average pressure of numerical simulation, ρ is the density of water, H is the head.

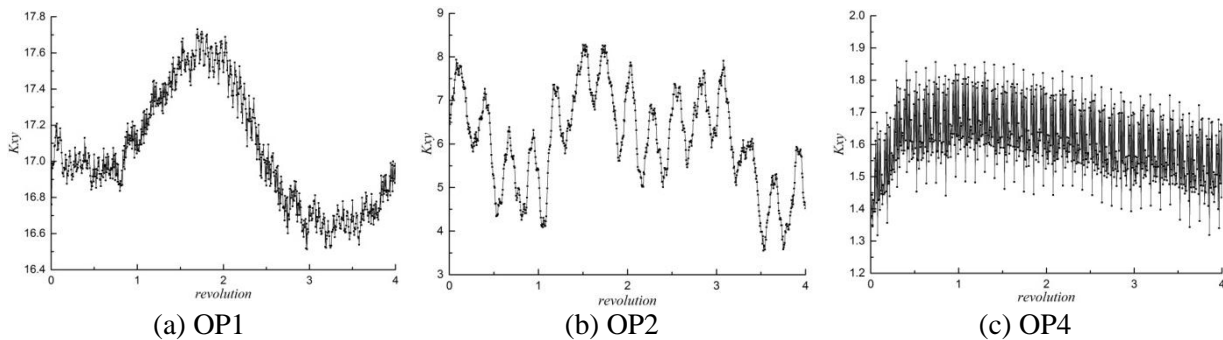


Figure 6. Time domain distribution

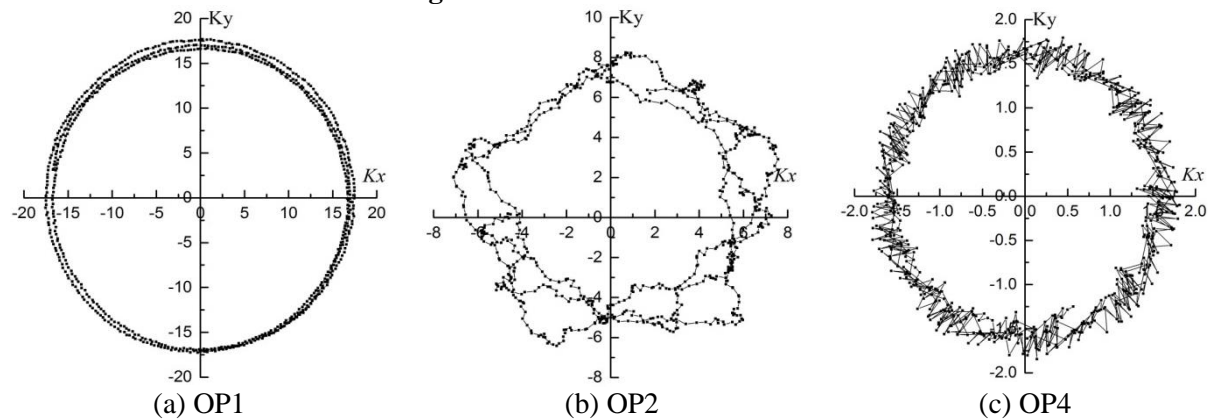
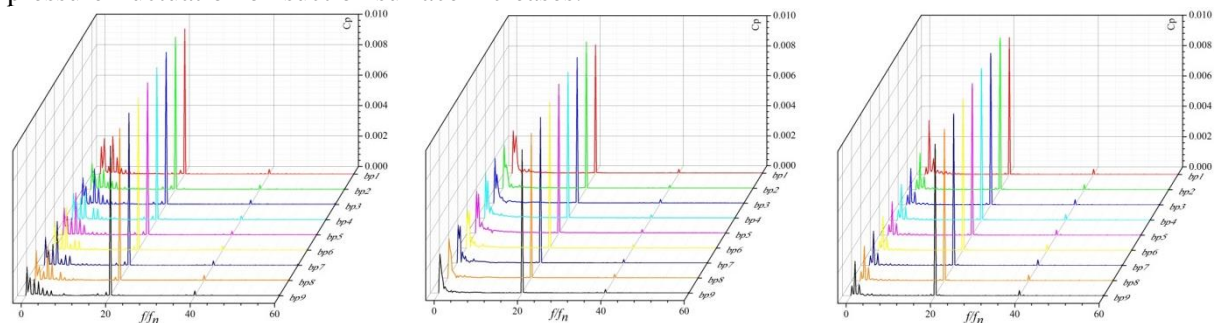


Figure 7. Vectorgraph of radial force

The frequency domain of all monitor points is shown in Figure 8. In the pressure surface, the dominant frequency is $20f_n$ (rotating frequency), and it was caused by rotor stator. The amplitude on the pressure surface is bigger than suction surface. The flow separation is more obvious and there is more low frequency pressure fluctuation at small discharge condition. The dominant frequency on suction surface is $0.25f_n$ at OP1. With the decrease of discharge, the amplitude of low frequency pressure fluctuation on suction surface increases.



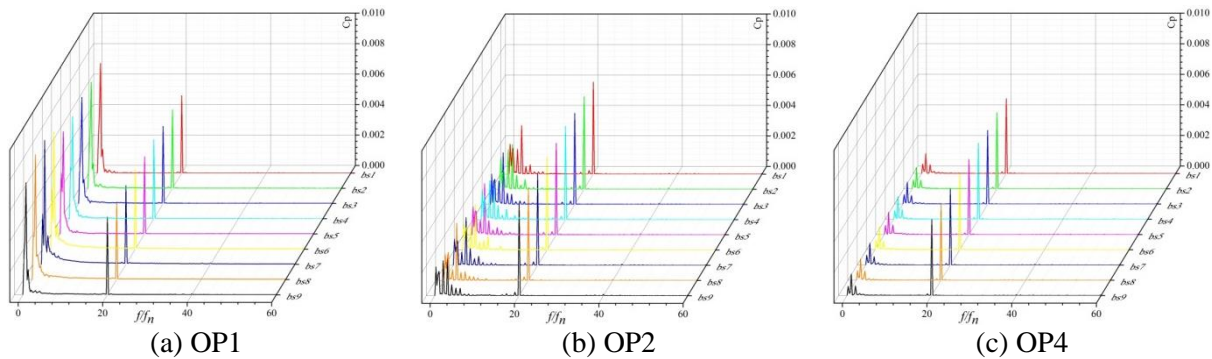


Figure 8. Pressure fluctuation frequency domain of all monitor points

The deviation coefficient of monitor points on the pressure surface is shown in Figure 9. For dominant frequency, the monitor point bp1 show great difference and it is bigger than other points. Because the location of this monitor point is near the tongue. For secondary frequency, S is bigger than dominant frequency. The value of S is almost 0.25 at bp2 and bp4, it fluctuated significantly and it is far away from average value at OP1.

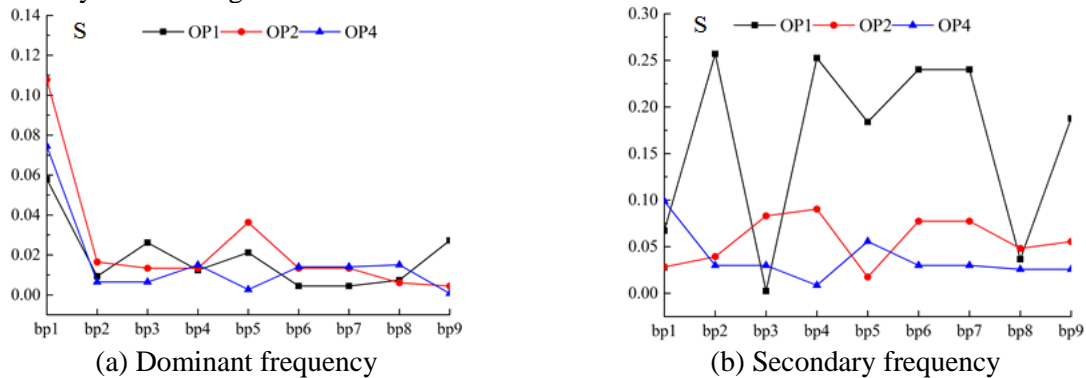


Figure 9. the deviation coefficient of amplitude on pressure surface

The deviation coefficient of monitor points on the suction surface is shown in and Figure 10. For dominant frequency, the S of all monitor points is very small. But for secondary frequency, the fluctuation of S is extremely volatile. Such as the minimum value is almost zero, but the maximum reached 0.2 at OP2.

To summarize, the low frequency and heterogeneity of pressure pulsation leads to the increase of radial force at partial load condition.

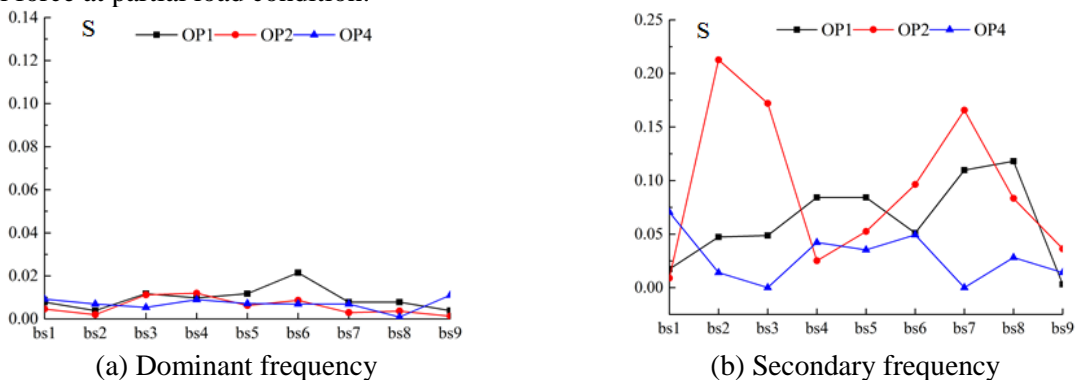


Figure 10. the deviation coefficient of amplitude on suction surface

5. Conclusion

The comprehensive calculation of pump turbine at partial load condition is carried out in this paper by using the numerical simulation method. And the analysis of hydraulic force and pressure fluctuation

was also carried out. Comparison and analysis of calculation results of different calculation conditions were conducted, and the following conclusions can be drawn:

(1) Axial force will increase significantly when the unit overloaded, it has almost no change at part load conditions. For the radial force, it is very small at the rated operating point. However the radial force increases sharply when the condition deviates from the rated operating point. With the increase of the flow rate, the axial force of the hub and shroud tends to decrease first and then increase, and the axial force on the runner is mainly produced by the hub and shroud, the axial force on the blade can be ignored.

(2) The runner rotated almost four revolutions but one revolution of radial force at OP1, and the radial force shows the characteristics of high frequency fluctuation at OP4.

(2) The frequency of pressure fluctuation is $20f_n$ which is caused by rotor stator. There is more low frequency pressure fluctuation at small discharge condition because of the flow separation. And the amplitude increased.

(3) The deviation coefficient of monitor point bp1 which location near the tongue is bigger than other points. The S of all monitor points dominant frequency on suction surface is very small. But for secondary frequency, the fluctuation of S is extremely volatile at partial load condition.

(4) The low frequency and heterogeneity of pressure pulsation leads to the increase of radial force at partial load condition. It will cause more vibration and threaten the safe operation of the unit.

Acknowledgments

So long and thanks for all the supports from the National Natural Science Foundation of China (51679196, 51879216, 51339005).

References

- [1] S. E. He and Xi. Z Dong. 2012 Cause analysis on large-scale wind turbine tripping and its countermeasures. *Power System Protection & Control* 131-137.
- [2] D Zhu, R F Xiao, R Tao, et al. 2016 Analysis of Flow regime and Pressure Pulsations under Off-design Condition in Pump Mode of Pump-turbine. *Transactions of the Chinese Society for Agricultural Machinery* 47(12)77-84
- [3] E Egusquiza, C Valero, D Valentin et al. 2015 Condition monitoring of pump turbines. New challenges. *Measurement* 67,151-163.
- [4] J W Li, Y N Zhang and K H Liu. 2017 Numerical simulation of hydraulic force on the impeller of the reversible pump turbine in generating mode *Journal of Hydrodynamics* 29(4)603-609
- [5] Q F Li, M M Liu, Q Liu, et al. 2017 Analysis of forces on runner and blades of pump turbine under braking condition *Journal of Drainage and Irrigation Machinery Engineering* 35(7)588-595
- [6] Q F Li, Z J Zhang, R N Li, et al. 2018 Analysis of Cavitation Performance and Force on Runner of Pump-turbine in Pump Mode *Transactions of the Chinese Society for Agricultural Machinery* 19(1)137-142
- [7] Y Zhang, T Chen, J Li, et al. 2017 Experimental study of load variations on pressure fluctuations in a prototype reversible pump turbine *Journal of Fluids Engineering* 139(7)074501.
- [8] Vlad Hasmatuchi. 2012 Hydrodynamics of a pump-turbine operating at off-design conditions in generating mode. EPFL
- [9] M Zhang, H Tsukamoto 2005 Unsteady hydrodynamics forces due to rotor-stator interaction on a diffuser pump with identical number of vanes on the impeller and diffuser *Journal of Fluids Engineering* 127(4)743-751
- [10] L K Wang, W L Liao and J L Lu, et al. 2017 Pressure fluctuations in pump turbines in S zone based on weakly compressible modelling. *Journal of Hydroelectric Engineering*. 36(6) 69-78